## MATERIALS AND METHODS

### General

Chemical reagents and solvents were from Millipore Sigma (St. Louis, MO) and used without further purification unless otherwise stated. DOTA was from Macrocyclics (Dallas, TX). Water was purified using Milli-Q ultra-pure water system from Millipore (Milford, MA). All solvents were HPLC grade from Sigma-Aldrich (St. Louis MO, USA).

### Bioreagents Source

MHC-II antibody was purchased from BioXCell (#BE0108). Rat IgG2b isotype antibody was purchased from BioXCell(#BE0090). PD1 antibody was purchased from BioXCell (#BE0273). IFNγ was purchased from Thermo Fisher Scientific (#PMC4033). Texas Red anti-rat IgG was purchased from Thermo Fisher Scientific (#T-6392). BCA Protein Assay was obtained from Thermo Fisher Scientific (#23227).

### Blocking Studies for PET Imaging

Two control PET imaging studies were performed to validate the specificity of the radiotracer with the following blocking agents: (a) non-radiolabled MHC-II antibody and (b) non-radiolabeled rat IgG2b isotype control. Specifically, cohort of B16SIY tumor-bearing mice were used in the blocking studies. Imaging, MHC-II blocking and IgG blocking were performed on three separate cohorts (n =5 per cohort). The study was performed when tumors reached ~600 $mm^3$. For imaging group, approximate 3.7 MBq $^{64}$Cu-DOTA-MHCII was intravenously injected into each tumor-bearing mouse, and in-line PET and CT scans were acquired at 48 h post injection (p.i.). For MHC-II blocking group, 200 μg non-radiolabeled MHC-II antibody was intravenously injected into each tumor-bearing mouse. After 30 minutes p.i. of blocking agent, approximate 3.7 MBq $^{64}$Cu-DOTA-MHCII was intravenously injected into each tumor-bearing mouse, and in-line PET and CT scans were acquired at 48 h p.i. Similarly, 200 μg non-radiolabeled IgG isotype antibody was intravenously injected into each tumor-bearing mouse 30 minutes prior to the injection of the radiotracer. The radiotracer dosage was similarly as approximate 3.7 MBq, and PET/CT images were acquired at 48 p.i. PET/CT image fusion was performed with the Inveon Research Workplace. For each PET scan, regions of interest (ROIs) were drawn over the tumor on decay-corrected

whole-body coronal images to derive tumor accumulation of the MHC-II immuno-PET imaging agent. The radioactivity concentration (accumulation) within tumor or organs was obtained from mean pixel values within the ROI volume and was converted to counts per milliliter per minute. Assuming a tissue density of 1 g/ml, the counts per milliliter per minute was converted to counts per gram per minute and then divided by the injected dose (ID) to obtain an imaging ROI-derived percentage of the injected radioactive dose per gram of tissue (%ID/g).

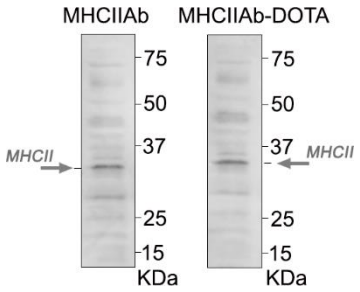


**Supplemental Figure 1.** Western blot of MHC-II antibody and the DOTA conjugate on protein extracts from MHC-II positive tumor tissue. No difference was observed on the immunoreactivity of the antibody and the DOTA conjugate.

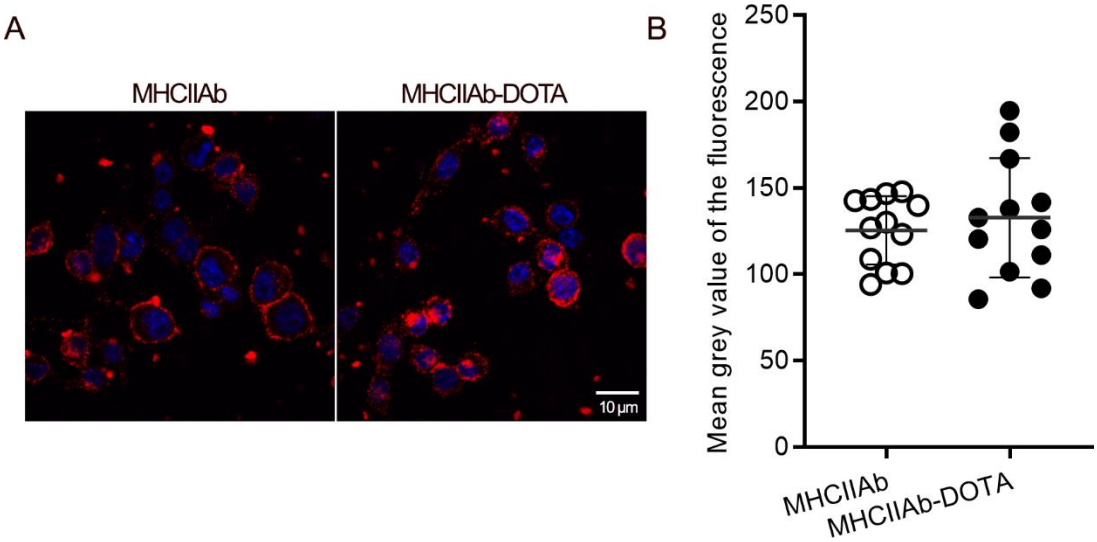


**Supplemental Figure 2.** Immunofluorescence staining of MHC-II antibody and the DOTA conjugate on a DC2.4 mouse dendritic cell line which typically presents antigen with high MHC-II positivity. The staining was imaged with confocal fluorescence microscopy (A). The mean fluorescence intensity in (A) was quantified and statistically analyzed to compare the significant

difference (B). No significant difference was observed among the antibody and its DOTA conjugate.

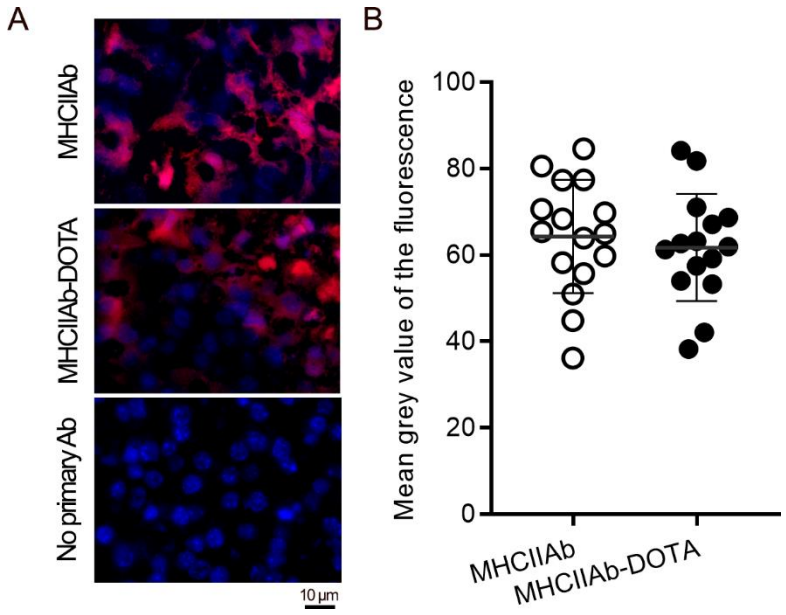


**Supplemental Figure 3.** MHC-II antibody immunofluorescence staining and the DOTA conjugate on B16SIY tumor tissue slides, with known MHC-II positivity. The staining was imaged with fluorescence microscopy (A). The mean fluorescence intensity in (A) was quantified and statistically analyzed to compare the significant difference (B). No significant difference was observed between the antibody and its DOTA conjugate.

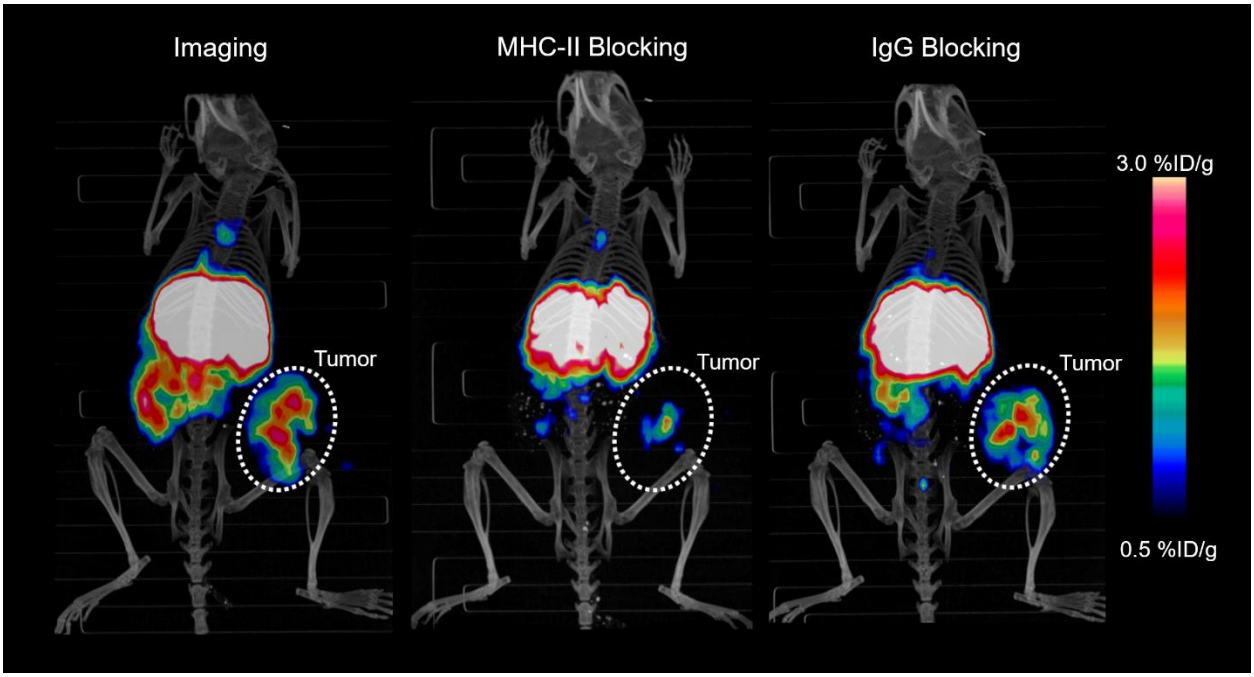


**Supplemental Figure 4.** Noninvasive PET-CT images of B16SIY tumor-bearing mice in the blocking studies. Two types of blocking were performed: (a) excessive non-radiolabeled MHC-II antibody (MHC-II Blocking); (b) excessive rat IgG2b isotype control (IgG Blocking). The blocking agent was injected 30 minutes prior to the injection of $^{64}$Cu-DOTA-MHCII radiotracer. The PET-CT image scan was performed after 48 hours injection of the radiotracer. The blocking imaging was compared to the imaging group with only radiotracer administrated (Imaging).

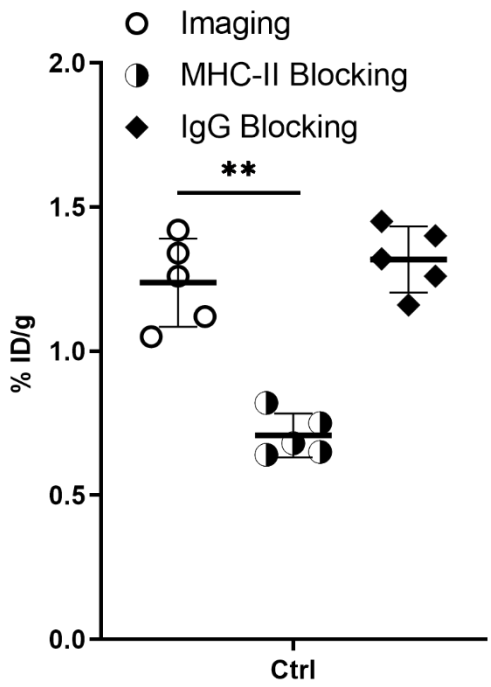


**Supplemental Figure 5.** ROI quantification of tumor accumulated $^{64}$Cu-DOTA-MHCII in PET images (n = 5 per group). Three groups were analyzed and compared: imaging group with only radiotracer administrated (Imaging); blocking study with excessive non-radiolabeled MHC-II antibody administrated prior to injection of the radiotracer (MHC-II Blocking); blocking study with excessive rat IgG2b isotype control administrated prior to injection the radiotracer (IgG Blocking). An unpaired student t test was performed to compare: MHC-II Blocking vs. Imaging (**, $P$ = 0.00126).

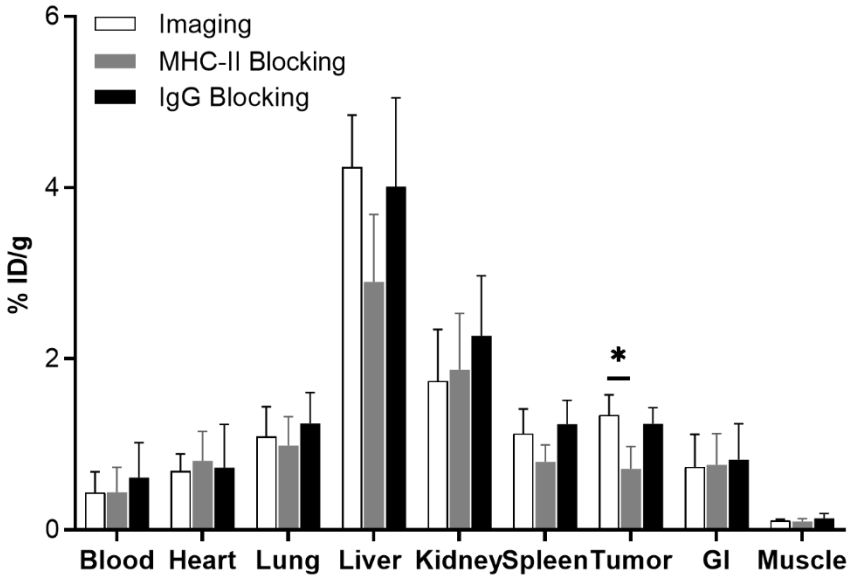


**Supplemental Figure 6.** Biodistribution of $^{64}$Cu-DOTA-MHCII in the PET blocking studies. Three groups were analyzed and compared: imaging group with only radiotracer administrated (Imaging); blocking study with excessive non-radiolabeled MHC-II antibody administrated prior to injection of the radiotracer (MHC-II Blocking); blocking study with excessive rat IgG2b isotype control administrated prior to injection the radiotracer (IgG Blocking). An unpaired student t test was performed to compare: MHC-II Blocking vs. Imaging (*, $P = 0.0283$). Gastrointestinal is abbreviated as GI.